

Published in final edited form as:

*Depress Anxiety*. 2014 October ; 31(10): 880–892. doi:10.1002/da.22291.

## Childhood maltreatment and combat post-traumatic stress differentially predict fear-related fronto-subcortical connectivity

Rasmus M Birn, PhD<sup>#1,2</sup>, Rémi Patriat, MS<sup>#2</sup>, Mary L Phillips, MD, MD<sup>3</sup>, Anne Germain, PhD<sup>3</sup>, and Ryan J Herringa, MD, PhD<sup>1,3</sup>

<sup>1</sup>Psychiatry, University of Wisconsin School of Medicine & Public Health, Madison, WI;

<sup>2</sup>Medical Physics, University of Wisconsin School of Medicine & Public Health, Madison, WI;

<sup>3</sup>Psychiatry, University of Pittsburgh School of Medicine, Pittsburgh, PA;

# These authors contributed equally to this work.

### Abstract

**Background**—Adult post-traumatic stress disorder (PTSD) has been characterized by altered fear network connectivity. Childhood trauma is a major risk factor for adult PTSD, yet its contribution to fear network connectivity in PTSD remains unexplored. We examined, within a single model, the contribution of childhood maltreatment, combat exposure, and combat-related post-traumatic stress symptoms (PTSS) to resting-state connectivity (rs-FC) of the amygdala and hippocampus in military veterans.

**Methods**—Medication-free male veterans (n=27, average 26.6 years) with a range of PTSS completed resting-state fMRI. Measures including the Clinician-Administered PTSD Scale (CAPS), Childhood Trauma Questionnaire (CTQ), and Combat Exposure Scale (CES) were used to predict rs-FC using multi-linear regression. Fear network seeds included the amygdala and hippocampus.

**Results**—Amygdala: CTQ predicted lower connectivity to ventromedial prefrontal cortex (vmPFC), but greater anticorrelation with dorsal/lateral PFC. CAPS positively predicted connectivity to insula, and loss of anticorrelation with dorsomedial/dorsolateral (dm/dl)PFC.

**Hippocampus**—CTQ predicted lower connectivity to vmPFC, but greater anticorrelation with dm/dlPFC. CES predicted greater anticorrelation, while CAPS predicted less anticorrelation with dmPFC.

**Conclusions**—Childhood trauma, combat exposure, and PTSS differentially predict fear network rs-FC. Childhood maltreatment may weaken ventral prefrontal-subcortical circuitry important in automatic fear regulation, but, in a compensatory manner, may also strengthen dorsal prefrontal-subcortical pathways involved in more effortful emotion regulation. PTSD symptoms, in turn, appear to emerge with the loss of connectivity in the latter pathway. These findings

---

Corresponding author: Ryan J. Herringa, Department of Psychiatry, University of Wisconsin School of Medicine & Public Health, 6001 Research Park Blvd., Madison, WI 53719, USA. herringa@wisc.edu. Phone: 608-263-6068..

Conflicts of interest: Dr. Germain has served as a consultant for Concurrent Technologies Corporation. The other authors report no biomedical financial interests or potential conflicts of interest.

suggest potential mechanisms by which developmental trauma exposure leads to adult PTSD, and which brain mechanisms are associated with the emergence of PTSD symptoms.

## Keywords

Abuse; maltreatment; brain imaging; functional MRI; PTSD; trauma

## Introduction

Neuroimaging studies of adult post-traumatic stress disorder (PTSD) suggest abnormalities in frontosubcortical circuitry underlying the regulation of fear responses. Relatively common findings include increased activation of the amygdala, insula, and dorsal anterior cingulate cortex (dACC), and relative hypoactivation of the ventromedial prefrontal cortex (vmPFC) in response to emotional stimuli<sup>1,2</sup>. The hippocampus shows increased activation to emotional stimuli, but impaired recruitment during fear extinction in subjects with PTSD<sup>1,3</sup>. The dACC and vmPFC appear to have opposing roles in the regulation of fear via the amygdala (facilitation and inhibition, respectively)<sup>4</sup>, while the hippocampus contextually regulates fear responses via the amygdala and vmPFC<sup>5</sup>. Within this framework, neural models of PTSD posit disrupted communication between the amygdala and hippocampus, and prefrontal regulatory areas, leading to exaggerated and generalized fear responses<sup>2,5</sup>.

Studies of resting state functional brain connectivity (rs-FC) in PTSD have yielded variable results but suggest altered connectivity of both the amygdala and hippocampus (see Table 1 for a summary of prior rs-FC studies involving the amygdala, hippocampus, and/or prefrontal areas). Compared to trauma-exposed controls, subjects with PTSD show greater connectivity of the amygdala with the insula<sup>6-8</sup>, lower connectivity with the hippocampus<sup>7</sup>, and reduced anticorrelation with pregenual (pg)/dACC<sup>7</sup>. Some of these differences may be specific to amygdala subnuclei, as evidenced by a recent study showing reduced anticorrelation between the basolateral amygdala (BLA) and the pgACC/dorsomedial (dm)PFC and dACC, and lower connectivity with the inferior frontal gyrus in PTSD subjects<sup>9</sup>. In contrast, there were no significant group differences in centromedial amygdala (CMA) connectivity. To date, only one reported study has examined rs-FC of the hippocampus in PTSD. Relative to non-trauma controls, PTSD subjects had lower connectivity between the anterior hippocampus and dACC/pre-supplementary motor area, and lower connectivity between the posterior hippocampus and pgACC and posterior cingulate/precuneus<sup>10</sup>. While the results of these studies vary, they appear to suggest that PTSD is characterized by lower dorsal/medial prefrontal-subcortical rs-FC, a pathway that is important in effortful emotion regulation<sup>11</sup>. On the other hand, there is little evidence for impaired ventral prefrontal-subcortical rs-FC, a pathway important in the automatic regulation of fear and emotion<sup>4,11</sup>.

The contribution of childhood maltreatment to altered rs-FC of the amygdala and hippocampus in PTSD remains unexplored but may explain some of the above discrepancies. A history of childhood trauma is one of the largest risk factors for adult PTSD, with an effect size comparable to the adult index trauma<sup>12</sup>. Although analytic approaches and study samples vary, prior rs-FC studies suggest that childhood maltreatment

or early life stress may alter amygdala and hippocampus connectivity in ways that create vulnerability for developing PTSD as an adult (see Table 1 for a summary). Using seed-based approaches, childhood maltreatment/early life stress has been associated with lower connectivity between the amygdala and insula/hippocampus<sup>13</sup>, lower connectivity between the amygdala and vmPFC<sup>14,15</sup>, and lower connectivity between the hippocampus and vmPFC<sup>15</sup>. Lower amygdala-vmPFC and hippocampus-vmPFC connectivity also mediated the development of internalizing symptoms by late adolescence, suggesting these changes create vulnerability for psychopathology<sup>14,15</sup>. Using graph theory approaches, childhood maltreatment/early life stress has been associated with decreased global connectivity of the amygdala, hippocampus, and PFC<sup>16</sup>, and decreased local connectivity and increased hub-like properties of the amygdala<sup>17</sup>. In contrast, resilience to childhood trauma has been associated with increased global connectivity of the hippocampus at rest<sup>17</sup>. Taken together, these findings suggest that childhood trauma exposure may weaken fear regulatory circuitry particularly in ventral prefrontal-subcortical pathways, creating a vulnerable brain substrate for the development of adult PTSD.

Here we examined, using a within-subjects design, how childhood maltreatment, combat exposure, and combat post-traumatic stress symptoms (PTSS) predict resting-state connectivity of the amygdala and hippocampus in medication-free, young military veterans. This study expands on prior rs-FC studies of PTSD in several important ways. First, we employed a dimensional approach to examine the neural correlates of PTSS (both above and below the PTSD threshold), which offers greater specificity to PTSD symptoms. Second, we included continuous measures of adult trauma (combat exposure) and childhood trauma within the same model to examine their relative contributions to brain connectivity. Prior rs-FC of PTSD have not included childhood or adult trauma exposure as covariates, though some have tried to control for adult trauma (combat exposure) by contrasting with a healthy combat-exposed group. Finally, this study uses a within-subjects design which is less likely to be affected by confounding variables that may influence group contrasts. Our primary hypotheses were that childhood trauma would predict lower amygdala-vmPFC and hippocampal-vmPFC connectivity, while adult trauma would predict greater hippocampal-vmPFC connectivity as an adaptive mechanism<sup>18</sup>. We expected that PTSS, and possibly adult trauma, would predict loss of anticorrelation between the amygdala/hippocampus and dorsal prefrontal areas including pgACC, dmPFC, and dACC, and greater amygdala-insula connectivity given findings from previous resting-state studies of PTSD.

## Method

### Participants

Twenty-eight combat veterans (all males, right-handed;  $26.6 \pm 2.6$  years, and previously described<sup>19</sup>) from Operations Enduring and Iraqi Freedom were recruited from ongoing studies to participate in this study. Prior military service information was obtained by DD Form 214 documentations. One subject was unable to complete the scan due to back discomfort, leaving 27 subjects in the final analysis. All participants were non-medicated for at least three weeks (2 months for fluoxetine) at the time of the study. Written informed consent was obtained following the University of Pittsburgh Institutional Review Board

guidelines. Exclusion criteria included active substance abuse (past month), suicidality, psychotic or bipolar disorder, MRI contraindication or neurological disease. In addition, participants were excluded if they were currently receiving treatment for traumatic brain injury (TBI) or had concussive symptoms at the time of the study. Of the 27 participants, 12 (44.4%) reported exposure to blast, fire or explosion. Eight participants (29.6%) reported a history of closed head injury, and two of them also endorsed a loss of consciousness during deployment. Six of these participants endorsed being dazed, confused or “seeing stars”, two endorsed not remembering the injury, and four endorsed having symptoms of concussion afterward. Symptoms included headache, dizziness and irritability. However, none had concussive symptoms or were being treated for any sequelae of TBI at the time of participation. Seventeen subjects met full criteria for current PTSD (past month) using the F1/I2 criteria of the Clinician-Administered PTSD scale (CAPS)<sup>20,21</sup>. PTSD symptoms for all subjects were related to combat and not childhood maltreatment experiences.

### Behavioral and clinical measures

In addition to the CAPS, the Structured Clinical Interview for DSM-IV Axis I Disorders (SCID-I) was conducted to examine current and past psychiatric diagnoses<sup>22</sup>. Three subjects met criteria for current major depressive disorder. Subjects were free of other current comorbid psychiatric disorders. Past DSM-IV diagnoses included major depressive disorder (n=4), bulimia nervosa (n=1), alcohol abuse/dependence (n=14), cannabis abuse/dependence (n=4), and cocaine abuse/dependence (n=1). The prevalence of these diagnoses did not significantly differ between PTSD and non-PTSD subjects (Chi-squared test,  $p = 0.09$ ). The Beck Depression Inventory (BDI)<sup>23</sup> was utilized to measure depressive symptom severity. The Combat Exposure Scale (CES)<sup>24</sup> was used to assess the level of combat exposure. Childhood maltreatment history was quantified using the Childhood Trauma Questionnaire (CTQ)<sup>25</sup>, which yields a continuous measure of childhood maltreatment experiences based on a Likert rating scale for each item. IQ was estimated using the National Adult Reading Test (NART)<sup>26</sup>. Table S1 summarizes the different demographic, behavioral, clinical measures, and their correlations.

### Data Acquisition

Functional and structural scans were acquired using a 3T Siemens Trio MRI scanner. Functional data were acquired using a 5.5 minute FAIR-QUIPSSII sequence: oblique acquisition, TE=18 ms, TR=4000 ms, TI1=700 ms, TI2=1000 ms, FOV=240×240 mm, 3.75×3.75 mm<sup>2</sup> in-plane resolution, slice thickness=6 mm, 21 slices. This pulse sequence can provide simultaneous estimates of cerebral blood flow and blood oxygenation level dependent (BOLD) signal. For the current study, we use only the BOLD signal, processed in a manner described below. Recent work has demonstrated that BOLD measures derived from arterial spin labeling scans provide similar measures of functional connectivity as data acquired with conventional BOLD fMRI acquisition<sup>27</sup>. Structural brain data were obtained using an axial T1-weighted MPRAGE sequence: TR=2.2s, TE=3.29ms, TI=1s, FOV 256×192mm, flip angle= 9 degrees, voxel size=1×1×1 mm, 192 slices.

## Preprocessing

All preprocessing and analysis were carried out using Analysis of Functional NeuroImages (AFNI)<sup>28</sup>, unless otherwise specified. BOLD signal was extracted from the acquired ASL data by adding to each time point the average ASL signal from the neighboring time points (3dcalc)<sup>29</sup>.

For preprocessing, the EPI images were first despiked (3dDespike)<sup>30</sup>, and image time series were registered in time using a 6-parameter (rigid-body) alignment to correct for subject motion (3dvolreg). Resulting BOLD resting scans were aligned to the anatomical scan and the outcome was checked visually to ensure that no obvious misalignment was present (`align_epi_anat.py` and `@Align_Centers`). The anatomy was converted to standard Talairach-Tournoux space and resampled to a 2×2×2 mm grid (`@auto_t1rc`). This transformation was applied to the BOLD resting scans (`adwarp`). The first four volumes of the resting-state scans were ignored to account for T1 saturation effects. Cerebrospinal fluid (CSF), grey and white matter segmentation were performed on each subject's anatomical scan using the "fast" routine from the FMRIB Software Library (FSL)<sup>31–33</sup>. White matter and CSF masks were resampled to the resting scan's grid (3dresample). The CSF mask was eroded once in each direction to ensure that the voxels present in the mask would only overlap with voxels representing primarily CSF on the resting scan. The white matter mask was eroded twice to make sure that very little grey matter signal would be included in the final white matter mask. The final white matter and CSF eroded masks were used to create nuisance regressors by extracting the average time series over each of those masks (3dROIstats). These average time series along with the six motion parameters were entered as nuisance variables in a regression model to remove their effect on the resting data, keeping the residual time series (3dDeconvolve). Resting data were then temporally filtered (3dBandpass) to ignore signal frequencies <0.01Hz and >0.1Hz. Finally, resting scans were spatially smoothed with a FWHM of 6 mm (3dmerge).

## Resting State Connectivity Analysis

Resting state connectivity analyses were performed using a seed-based (region-of-interest or ROI) approach. For our primary analyses, we used four ROIs: left and right amygdala (Talairach LPI coordinates: -23, -6, -20 and 21, -6, -20, respectively), and left and right hippocampus (-31, -25, -11 and 29, -25, -11, respectively). AFNI was used to generate 4mm spheres centered on the above coordinate locations provided by the Talairach Daemon<sup>34,35</sup>. All seeds were resampled to the resolution of the resting-state EPIs (3dresample) and average time series were computed for each seed (3dmaskave). Connectivity maps were generated for each subject and each seed using a linear regression (3dDeconvolve). To facilitate comparison with prior rs-FC studies of PTSD, we also conducted supplementary seed-based analyses using amygdala<sup>9</sup> and hippocampal<sup>10</sup> subdivisions, as well as anterior insula<sup>8</sup>. These analyses are further described in the supplemental materials.

At the group level and for each seed independently, a multivariate regression analysis was conducted (3dttest++) to generate group-level connectivity maps for the above-mentioned seeds including CAPS, CES, and CTQ scores. Correlation coefficients were converted to Z-scores using Fisher's-Z transformation. Multiple comparison correction was performed

using Monte Carlo simulation (3dClustSim), which incorporates the estimated smoothness of the data to establish the likelihood of false positives of different cluster sizes (i.e. cluster size thresholding)<sup>36</sup>. The cluster threshold was 357 voxels ( $2 \times 2 \times 2\text{mm}^3$ ) at an individual voxel threshold of  $p = 0.005$ , resulting in a corrected  $\alpha = 0.05$ .

## Results

For the following multivariate regression analyses, relationships between the variable of interest and residualized connectivity (adjusted for other variables in the model) are shown in the figures as indicated. Relationships between the variable of interest and raw connectivity scores can be seen in Figure S1 (supplementary material).

### Resting state connectivity

Figure 1 shows the connectivity maps for left amygdala and hippocampus (threshold:  $p = 0.005$ ). Connectivity maps for right amygdala and hippocampus were similar. The left and right amygdala showed positive functional connectivity to each other as well as the insula, ventral striatum, hippocampus, parahippocampal gyrus, and medial frontal gyrus, and negative connectivity to posterior cingulate and occipital cortex. The left and right hippocampus showed positive connectivity with each other as well as other regions including the lentiform nucleus, insula, and thalamus. Connectivity maps for amygdala and hippocampal subdivisions are described in the supplemental text and displayed in Figures S2 and S3, respectively.

### Correlation with childhood maltreatment (CTQ total score)

**Amygdala Connectivity**—CTQ negatively predicted connectivity from left and right amygdala to mPFC including vmPFC/rostral (r)ACC and dorsomedial (dm)PFC (BA 9, 10, 32; Figure 2a), indicating more negative residualized connectivity with higher CTQ (see scatter plots, Fig. 2a). In addition, CTQ negatively predicted connectivity between left amygdala and lateral PFC including both ventrolateral (vl) and dorsolateral (dl) PFC (BA 9, 10, 47; Table 1). Like the mPFC clusters, this association indicated more negative residualized connectivity with higher CTQ scores. Finally, CTQ positively predicted connectivity from left and right amygdala to cerebellum (Table 1). Supplementary analyses of the CMA and BLA seeds revealed overall similar patterns to the primary amygdala seed. In this case, CTQ negatively predicted connectivity from CMA and BLA to mPFC areas including vmPFC/rACC and dmPFC (Figure S4ab, Table S2). However, the negative association of CTQ with connectivity to lateral PFC (specifically dlPFC) was only present for the BLA (Table S2).

**Hippocampus connectivity**—CTQ negatively predicted connectivity from left and right hippocampus to mPFC including vmPFC/rACC/dmPFC (BA 9, 10, 32; Figure 2b) indicating more negative residualized connectivity with higher CTQ scores. Additionally, CTQ negatively predicted connectivity between right hippocampus and dlPFC (BA 9, 10, 46; Table 1), indicating more negative connectivity with higher CTQ scores. Finally, CTQ positively predicted connectivity from left and right hippocampus to PCC/Precuneus (BA 30, 31), and left hippocampus to cerebellum (Table 1). Supplementary analyses of the



anterior and posterior hippocampal seeds revealed overall similar connectivity results to the primary hippocampus seed in relation to CTQ scores (Figure S4c-d, Table S2).

### Correlation with combat exposure (CES)

**Amygdala connectivity**—CES positively predicted connectivity between right amygdala and cerebellum (Table 1). No other significant associations were observed with left or right amygdala connectivity. In addition, no significant associations with CES were observed with CMA and BLA connectivity.

**Hippocampus connectivity**—CES negatively predicted connectivity between left hippocampus and dmPFC (BA 9, Figure 3), indicating less positive to more negative residualized connectivity with higher CES scores. Supplementary analyses of anterior and posterior hippocampus connectivity yielded similar results in relation to CES (Figure S5, Table S2).

### Correlation with PTSS (CAPS past month)

**Amygdala connectivity**—CAPS scores positively predicted connectivity between right amygdala and dmPFC/rACC (BA 9, 32; Figure 4a top panel), and between left amygdala and bilateral dlPFC (BA 10, 46, Figure 4a middle panel). This correlation indicated more positive residualized connectivity with higher CAPS scores. In addition, CAPS scores positively predicted connectivity between left amygdala and bilateral anterior insula (BA 13; Figure 4a bottom panel), indicating more positive residualized connectivity with higher CAPS scores. Finally, CAPS scores negatively predicted connectivity between left amygdala and cerebellum (Table 1). Supplementary analyses of the CMA and BLA yielded similar connectivity results in association with CAPS scores, with no clear differences between the amygdala subdivisions (Figure S6a-c, Table S2).

**Hippocampus connectivity**—CAPS scores positively predicted connectivity to dmPFC (BA 9, Figure 4b) indicating more positive residualized connectivity with higher CAPS scores. CAPS scores negatively predicted connectivity to PCC (BA 30, Table 1). Supplementary analyses of anterior and posterior hippocampus connectivity yielded similar results in relation to CAPS. However, the association with anterior hippocampus connectivity was more widespread in the mPFC with extension into dlPFC (Figure S6d, Table S2).

### Covariation for depressive symptoms and TBI history

To examine potentially confounding effects of depressive symptoms and TBI history in the current results, we conducted a secondary analysis of our primary variables of interest and resting state connectivity, with depressive symptoms (BDI) and lifetime TBI history (present or absent) included as an additional covariates in our model. Inclusion of these variables did not change the pattern of results with our primary variables.

## Discussion

In this study, we investigated resting state functional connectivity of the amygdala and hippocampus, two key fear network nodes, in young combat veterans with a wide range of PTSD symptoms. Importantly, we examined the relation of this connectivity not only to PTSD symptom severity but also to both adult and child trauma exposure within a single model. This represents an important step in identifying potential mechanisms by which developmental trauma exposure may lead to adult PTSD symptoms, and in turn which circuitry changes distinguish PTSD symptoms from trauma exposure itself.

### Amygdala

We found that childhood maltreatment negatively predicted connectivity between the amygdala and vmPFC, as well as connectivity between the amygdala and lateral PFC regions. The vmPFC and its rat homologue IL are notable for their role in the recall of fear extinction and down-regulation of amygdala-dependent fear responses<sup>4</sup>. The vmPFC is recruited during the recall of fear extinction in healthy individuals<sup>37,38</sup>, and the magnitude of activation is correlated with extinction retention<sup>39</sup>. In addition, resting amygdala metabolism negatively predicts vmPFC activation during extinction recall<sup>40</sup>, which suggests that communication between these regions plays an important role in human fear extinction. Consistent with this regulatory role, greater functional connectivity between amygdala and vmPFC is linked to lower anxiety levels during presentation of fearful faces<sup>41</sup> and at rest<sup>42</sup> in healthy individuals. In agreement with the current results, our prior work revealed that early life stress and childhood maltreatment are associated with weaker amygdala-vmPFC connectivity, which in turn predicts the development of internalizing symptoms<sup>14,15</sup>. Thus, our data support a model in which childhood maltreatment experiences may weaken this key automatic fear regulatory circuit, which may contribute risk towards the development of PTSD following subsequent trauma in adulthood. At the same time, a weakening of amygdala-vmPFC connectivity induced by childhood maltreatment does not appear sufficient in and of itself to account for the emergence of PTSD symptoms, which instead are associated with a loss of amygdala connectivity to more dorsal prefrontal areas as described below.

In contrast to childhood maltreatment exposure, PTSS predicted a loss of anticorrelation between the amygdala and dorsal PFC regions including dmPFC/rACC and dlPFC. These dorsal PFC areas are notable for their role in effortful top-down emotion regulation, and appear to exert their regulatory influence on the amygdala via the vmPFC<sup>11,43</sup>. In healthy individuals, dorsal PFC regions are anticorrelated with the amygdala during task and rest<sup>42,44,45</sup>. Furthermore, successful emotion regulation is associated with greater amygdala-dm/dlPFC anticorrelation during task<sup>46</sup>, and higher anxiety levels are associated with a loss of resting amygdala-dmPFC anticorrelation<sup>42</sup>. PTSD has also been characterized by reduced amygdala-dmPFC/rACC anticorrelation both during symptom provocation<sup>45</sup> and at rest<sup>7,9</sup>. Our results are consistent with these studies and, when examined in relation to raw (non-residualized) amygdala-dmPFC connectivity, suggest a loss of anticorrelation and a switch to positive connectivity with higher CAPS scores (see Fig. S1). Within this framework, childhood maltreatment may create a vulnerable brain substrate by weakening amygdala-



vmPFC connectivity, yet PTSD symptoms may only emerge with a subsequent loss of amygdala-dorsal PFC anticorrelation. Interestingly, childhood maltreatment negatively predicted amygdala-dorsal PFC connectivity (i.e. greater anticorrelation). This could be attributable to shared variance with vmPFC-amygdala connectivity (also negatively predicted by CTQ). Alternatively, our results suggest that greater amygdala-dorsal PFC anticorrelation represents a compensatory brain mechanism employing effortful emotion regulation following childhood maltreatment, the failure of which is associated with the emergence of PTSD symptoms. Ultimately, longitudinal studies examining both childhood and adult trauma exposure and adult PTSS, along with causality modeling<sup>47</sup> will be needed to tease apart these possibilities.

PTSS also positively correlated with resting amygdala-anterior insula connectivity. The anterior insula is involved in the representation of visceral emotional states<sup>48</sup> and has strong structural and functional connectivity with the amygdala<sup>49,50</sup>. As detailed in previous studies, greater connectivity at rest between these areas may represent heightened integration of threat and interoceptive processing that could underlie hyperarousal and re-experiencing phenomena of PTSD<sup>6,7</sup>. As such, these findings remain consistent with prior resting-state studies of PTSD and suggest specificity of changes in this circuit to PTSD symptoms.

## Hippocampus

We found that childhood maltreatment negatively predicted connectivity between the hippocampus and vmPFC, as well as dm/dlPFC. Combat exposure also negatively predicted hippocampus-PFC connectivity, though this was localized to the dmPFC. The hippocampus is known to play an important role in the regulation of fear by contextually limiting fear responses via connections to both the amygdala and vmPFC<sup>5</sup>. In rats, chronic stress impairs hippocampus-mPFC long-term potentiation, which is required for the proper gating of conditioned fear<sup>51,52</sup>. In humans, both the vmPFC and hippocampus are recruited during the recall of fear extinction, e.g.<sup>38,39</sup>, in support of their coordinated role in gating fear. Consistent with the current findings, prior work from our group has shown that childhood maltreatment is associated with weaker hippocampus-vmPFC connectivity, which in turn mediates the development of internalizing symptoms<sup>15</sup>. Within this framework, our findings suggest that childhood maltreatment in particular may weaken the contextual regulation of fear by impairing communication between the hippocampus and vmPFC, though this would require further testing in a fear conditioning paradigm. Of note, a longitudinal study revealed that adult trauma (combat exposure) actually increases hippocampus-vmPFC connectivity to emotional stimuli, and failure to increase this connectivity was associated with the development of PTSD symptoms<sup>18</sup>. Our results suggest that childhood maltreatment exposure could compromise the ability of this circuit to adaptively upregulate following adult trauma, placing an individual at risk for developing fear-related psychopathology as an adult.

In contrast to childhood maltreatment and similar to the amygdala findings, PTSS predicted a loss of anticorrelation between the hippocampus and dorsal PFC, specifically to dmPFC. In healthy individuals, the hippocampus and dmPFC show inverse patterns of activation in

signaling safety versus threat (i.e. hippocampus activation and dmPFC deactivation to safety cues, and vice versa to conditioned threat)<sup>53</sup>. Furthermore, PTSD subjects display hippocampus deactivation and dACC activation to extinguished threat cues<sup>3</sup>, suggesting a reversal of the pattern seen in healthy individuals. In light of this, the loss of resting dmPFC-hippocampus anticorrelation (and switch to positive connectivity) associated with PTSS in the current study could reflect impaired communication between the hippocampus and dmPFC in predicting safety versus threat. This suggests that the ability of the hippocampus to contextually regulate fear is further compromised in PTSD, involving a disruption in communication with dorsal prefrontal areas. Like the amygdala connectivity findings, childhood maltreatment may create a vulnerable brain substrate by reducing vmPFC-hippocampal connectivity, however, PTSD symptoms may only emerge with a subsequent loss of dmPFC-hippocampus anticorrelation. Interestingly, both childhood maltreatment and combat exposure negatively predicted dorsal PFC-hippocampus connectivity (i.e. greater anticorrelation), suggesting these may be compensatory attempts which are lost with the development of PTSS. As with the amygdala connectivity findings, longitudinal studies will ultimately be needed, along with causality modeling, to tease apart these possibilities.

Of note, we did not observe any marked dissociations of amygdala or hippocampal subdivisions in our results, in contrast to prior studies<sup>9,10</sup>. The reasons for this are not entirely clear but likely reflect different experimental designs (within-subjects vs. between-group analysis), analytic approaches (e.g. use of global signal regression and *a priori* search regions<sup>10</sup>), and the inclusion of the additional trauma variables in our study. Our study sample also differs from these prior studies in that we did not allow any current psychiatric medication usage. Further work will be needed, likely with larger sample sizes, to examine whether there are consistent and dissociable rs-FC findings among amygdala and hippocampal subdivisions in PTSD.

The results of this study underscore the utility of using resting-state fMRI to detect the neurobiological correlates of trauma exposure and PTSS. However, these results are not without limitations. First, these findings are correlational only and do not prove causation. It is thus difficult to tease out whether observed changes represent preexisting vulnerabilities, state-related changes, or compensatory changes. Second, these findings may not generalize to other populations (particularly women given the all-male sample), trauma types, or to individuals with more severe PTSS. In addition, resting state connectivity may not necessarily equate to task-related connectivity, an area which requires further study. Third, while subjects were free of current alcohol or substance abuse, this study did not have measures of cumulative, lifelong alcohol use, which could affect the current results. However, PTSD and non-PTSD subjects had similar frequencies of past alcohol abuse/dependence which makes this less likely. Finally, this is a moderate number of subjects with results considered preliminary, and would merit replication in a larger sample and using longer duration acquisitions. While 5-minutes of resting-state data have been used successfully in other studies to characterize differences in functional connectivity (e.g.<sup>54</sup>) and have moderate test-retest reliability<sup>55</sup>, more recent studies suggest that the reliability of these results would improve even further with longer duration acquisitions<sup>56</sup>.

## Conclusion

The results from this study suggest that childhood trauma, combat exposure, and combat-PTSS differentially predict resting-state connectivity of the amygdala and hippocampus, two key nodes in the fear network. Childhood trauma in particular may create a vulnerable brain substrate by weakening ventromedial prefrontal-subcortical pathways involved in the extinction and contextual gating of fear, yet may also be accompanied by compensatory strengthening of dorsal prefrontal-subcortical circuits involved in effortful emotion regulation. PTSS, in turn, may emerge upon this background with the loss of anticorrelation between dorsal prefronto-subcortical pathways, as well as greater fear/interoceptive processing involving the amygdala and insula. These findings highlight the importance of examining developmental trauma exposure and adult PTSS within a single model. They also represent an important step in identifying potential mechanisms by which developmental trauma exposure may lead to adult PTSD, and which mechanisms are associated with the emergence of PTSD symptoms themselves.

## Supplementary Material

Refer to Web version on PubMed Central for supplementary material.

## Acknowledgments

The authors would like to thank Benjamin Paul, Ashlee Filippone, and Ryan Stocker for their assistance with participant screening, MRI procedures, and data organization.

Funding: This work was supported by the AACAP Pilot Research Award (RJH), Department of Defense Congressionally Directed Medical Research Program PT073961 (AG), and the National Institute of Mental Health MH083035 (AG), MH076971 (MLP), MH088913 (MLP).

## References

1. Patel R, Spreng RN, Shin LM, Girard TA. Neurocircuitry models of posttraumatic stress disorder and beyond: a meta-analysis of functional neuroimaging studies. *Neurosci Biobehav Rev.* Oct; 2012 36(9):2130–42. [PubMed: 22766141]
2. Pitman RK, Rasmusson AM, Koenen KC, Shin LM, Orr SP, Gilbertson MW, et al. Biological studies of post-traumatic stress disorder. *Nat Rev Neurosci.* Nov; 2012 13(11):769–87. [PubMed: 23047775]
3. Milad MR, Pitman RK, Ellis CB, Gold AL, Shin LM, Lasko NB, et al. Neurobiological basis of failure to recall extinction memory in posttraumatic stress disorder. *Biol Psychiatry.* Dec 15; 2009 66(12):1075–82. [PubMed: 19748076]
4. Milad MR, Quirk GJ. Fear extinction as a model for translational neuroscience: ten years of progress. *Annu Rev Psychol.* Jan 10.2012 63:129–51. [PubMed: 22129456]
5. Maren S, Phan KL, Liberzon I. The contextual brain: implications for fear conditioning, extinction and psychopathology. *Nat Rev Neurosci.* Jun; 2013 14(6):417–28. [PubMed: 23635870]
6. Rabinak CA, Angstadt M, Welsh RC, Kenndy AE, Lyubkin M, Martis B, et al. Altered amygdala resting-state functional connectivity in post-traumatic stress disorder. *Front Psychiatry.* 2011; 2:62. [PubMed: 22102841]
7. Sripada RK, King AP, Garfinkel SN, Wang X, Sripada CS, Welsh RC, et al. Altered resting-state amygdala functional connectivity in men with posttraumatic stress disorder. *J Psychiatry Neurosci.* Feb 7.2012 37(2):110069.

8. Sripada RK, King AP, Welsh RC, Garfinkel SN, Wang X, Sripada CS, et al. Neural dysregulation in posttraumatic stress disorder: evidence for disrupted equilibrium between salience and default mode brain networks. *Psychosom Med.* Nov; 2012 74(9):904–11. [PubMed: 23115342]
9. Brown VM, Labar KS, Haswell CC, Gold AL, Mid-Atlantic MIRECC Workgroup. Beall SK, et al. Altered resting-state functional connectivity of basolateral and centromedial amygdala complexes in posttraumatic stress disorder. *Neuropsychopharmacology.* Jan; 2014 39(2):361–9.
10. Chen AC, Etkin A. Hippocampal network connectivity and activation differentiates post-traumatic stress disorder from generalized anxiety disorder. *Neuropsychopharmacology.* Sep; 2013 38(10): 1889–98. [PubMed: 23673864]
11. Phillips ML, Ladouceur CD, Drevets WC. A neural model of voluntary and automatic emotion regulation: implications for understanding the pathophysiology and neurodevelopment of bipolar disorder. *Mol Psychiatry.* Sep; 2008 13(9):829, 833–57. [PubMed: 18574483]
12. Brewin CR, Andrews B, Valentine JD. Meta-analysis of risk factors for posttraumatic stress disorder in trauma-exposed adults. *J Consult Clin Psychol.* Oct; 2000 68(5):748–66. [PubMed: 11068961]
13. Van der Werff SJA, Pannekoek JN, Veer IM, van Tol M-J, Aleman A, Veltman DJ, et al. Resting-state functional connectivity in adults with childhood emotional maltreatment. *Psychol Med.* Dec. 2012 20:1–12.
14. Burghy CA, Stodola DE, Ruttle PL, Molloy EK, Armstrong JM, Oler JA, et al. Developmental pathways to amygdala-prefrontal function and internalizing symptoms in adolescence. *Nat Neurosci.* Nov; 2012 15(12):1736–41. [PubMed: 23143517]
15. Herringa RJ, Birn RM, Ruttle PL, Burghy CA, Stodola DE, Davidson RJ, et al. Childhood maltreatment is associated with altered fear circuitry and increased internalizing symptoms by late adolescence. *Proc Natl Acad Sci USA.* Nov 19; 2013 110(47):19119–24. [PubMed: 24191026]
16. Wang L, Dai Z, Peng H, Tan L, Ding Y, He Z, et al. Overlapping and segregated resting-state functional connectivity in patients with major depressive disorder with and without childhood neglect. *Hum Brain Mapp.* Feb 13.2013
17. Cisler JM, James GA, Tripathi S, Mletzko T, Heim C, Hu XP, et al. Differential functional connectivity within an emotion regulation neural network among individuals resilient and susceptible to the depressogenic effects of early life stress. *Psychol Med.* 2013; 43(03):507–18. [PubMed: 22781311]
18. Admon R, Lubin G, Stern O, Rosenberg K, Sela L, Ben-Ami H, et al. Human vulnerability to stress depends on amygdala's predisposition and hippocampal plasticity. *Proc Natl Acad Sci USA.* Aug 18; 2009 106(33):14120–5. [PubMed: 19666562]
19. Herringa RJ, Phillips ML, Fournier JC, Kronhaus DM, Germain A. Childhood and adult trauma both correlate with dorsal anterior cingulate activation to threat in combat veterans. *Psychol Med.* Jul; 2013 43(7):1533–42. [PubMed: 23171514]
20. Blake DD, Weathers FW, Nagy LM, Kaloupek DG, Gusman FD, Charney DS, et al. The development of a Clinician-Administered PTSD Scale. *J Trauma Stress.* Jan; 1995 8(1):75–90. [PubMed: 7712061]
21. Weathers FW, Keane TM, Davidson JR. Clinician-administered PTSD scale: a review of the first ten years of research. *Depress Anxiety.* 2001; 13(3):132–56. [PubMed: 11387733]
22. First, MB.; Spitzer, RL.; Gibbon, M.; Williams, JBW. Structured Clinical Interview for DSM-IV-TR Axis I Disorders, Research Version, Patient Edition. (SCID-I/P). Biometrics Research, New York State Psychiatric Institute; New York: 2002.
23. Beck AT, Ward CH, Mendelson M, Mock J, Erbaugh J. An inventory for measuring depression. *ArchGenPsychiatry.* Jun.1961 4:561–71.
24. Keane T, Fairbank J, Caddell J, Zimering R, Taylor K, Mora C. Clinical evaluation of a measure to assess combat exposure. *Psychological assessment.* 1989; 1(1):53–5.
25. Scher CD, Stein MB, Asmundson GJ, McCreary DR, Forde DR. The childhood trauma questionnaire in a community sample: psychometric properties and normative data. *J Trauma Stress.* Oct; 2001 14(4):843–57. [PubMed: 11776429]
26. Blair JR, Spreen O. Predicting premorbid IQ: A revision of the national adult reading test. *Clinical Neuropsychologist.* 1989; 3(2):129–36.

27. Zhu S, Fang Z, Hu S, Wang Z, Rao H. Resting state brain function analysis using concurrent BOLD in ASL perfusion fMRI. *PLoS ONE*. 2013; 8(6):e65884. [PubMed: 23750275]
28. Cox RW. AFNI: software for analysis and visualization of functional magnetic resonance neuroimages. *Comput Biomed Res*. Jun; 1996 29(3):162–73. [PubMed: 8812068]
29. Wong EC, Buxton RB, Frank LR. Implementation of quantitative perfusion imaging techniques for functional brain mapping using pulsed arterial spin labeling. *NMR Biomed*. Aug; 1997 10(4-5): 237–49. [PubMed: 9430354]
30. Jo HJ, Gotts SJ, Reynolds RC, Bandettini PA, Martin A, Cox RW, et al. Effective Preprocessing Procedures Virtually Eliminate Distance-Dependent Motion Artifacts in Resting State FMRI. *J Appl Math*. May 21.2013 2013
31. Smith SM, Jenkinson M, Woolrich MW, Beckmann CF, Behrens TEJ, Johansen-Berg H, et al. Advances in functional and structural MR image analysis and implementation as FSL. *Neuroimage*. 2004; 23(Suppl 1):S208–219. [PubMed: 15501092]
32. Woolrich MW, Jbabdi S, Patenaude B, Chappell M, Makni S, Behrens T, et al. Bayesian analysis of neuroimaging data in FSL. *Neuroimage*. Mar; 2009 45(1 Suppl):S173–186. [PubMed: 19059349]
33. Zhang Y, Brady M, Smith S. Segmentation of brain MR images through a hidden Markov random field model and the expectation-maximization algorithm. *IEEE Trans Med Imaging*. Jan; 2001 20(1):45–57. [PubMed: 11293691]
34. Lancaster JL, Rainey LH, Summerlin JL, Freitas CS, Fox PT, Evans AC, et al. Automated labeling of the human brain: a preliminary report on the development and evaluation of a forward-transform method. *Hum Brain Mapp*. 1997; 5(4):238–42. [PubMed: 20408222]
35. Lancaster JL, Woldorff MG, Parsons LM, Liotti M, Freitas CS, Rainey L, et al. Automated Talairach Atlas labels for functional brain mapping. *Hum Brain Mapp*. 2000; 10(3):120–31. [PubMed: 10912591]
36. Forman SD, Cohen JD, Fitzgerald M, Eddy WF, Mintun MA, Noll DC. Improved assessment of significant activation in functional magnetic resonance imaging (fMRI): use of a cluster-size threshold. *Magn Reson Med*. May; 1995 33(5):636–47. [PubMed: 7596267]
37. Phelps EA, Delgado MR, Nearing KI, LeDoux JE. Extinction learning in humans: role of the amygdala and vmPFC. *Neuron*. Sep 16; 2004 43(6):897–905. [PubMed: 15363399]
38. Kalisch R, Korenfeld E, Stephan KE, Weiskopf N, Seymour B, Dolan RJ. Context-dependent human extinction memory is mediated by a ventromedial prefrontal and hippocampal network. *J Neurosci*. Sep 13; 2006 26(37):9503–11. [PubMed: 16971534]
39. Milad MR, Wright CI, Orr SP, Pitman RK, Quirk GJ, Rauch SL. Recall of fear extinction in humans activates the ventromedial prefrontal cortex and hippocampus in concert. *Biol Psychiatry*. Sep 1; 2007 62(5):446–54. [PubMed: 17217927]
40. Linnman C, Zeidan MA, Furtak SC, Pitman RK, Quirk GJ, Milad MR. Resting amygdala and medial prefrontal metabolism predicts functional activation of the fear extinction circuit. *Am J Psychiatry*. Apr; 2012 169(4):415–23. [PubMed: 22318762]
41. Pezawas L, Meyer-Lindenberg A, Drabant EM, Verchinski BA, Munoz KE, Kolachana BS, et al. 5-HTTLPR polymorphism impacts human cingulate-amygdala interactions: a genetic susceptibility mechanism for depression. *Nat Neurosci*. Jun; 2005 8(6):828–34. [PubMed: 15880108]
42. Kim MJ, Gee DG, Loucks RA, Davis FC, Whalen PJ. Anxiety dissociates dorsal and ventral medial prefrontal cortex functional connectivity with the amygdala at rest. *Cereb Cortex*. Jul; 2011 21(7):1667–73. [PubMed: 21127016]
43. Ghashghaei HT, Hilgetag CC, Barbas H. Sequence of information processing for emotions based on the anatomic dialogue between prefrontal cortex and amygdala. *Neuroimage*. Feb 1; 2007 34(3):905–23. [PubMed: 17126037]
44. Roy AK, Shehzad Z, Margulies DS, Kelly AMC, Uddin LQ, Gotimer K, et al. Functional connectivity of the human amygdala using resting state fMRI. *Neuroimage*. Apr 1; 2009 45(2): 614–26. [PubMed: 19110061]

45. Gilboa A, Shalev AY, Laor L, Lester H, Louzoun Y, Chisin R, et al. Functional connectivity of the prefrontal cortex and the amygdala in posttraumatic stress disorder. *Biol Psychiatry*. Feb 1; 2004 55(3):263–72. [PubMed: 14744467]
46. Lee H, Heller AS, van Reekum CM, Nelson B, Davidson RJ. Amygdala-prefrontal coupling underlies individual differences in emotion regulation. *Neuroimage*. Sep; 2012 62(3):1575–81. [PubMed: 22634856]
47. Sridharan D, Levitin DJ, Menon V. A critical role for the right fronto-insular cortex in switching between central-executive and default-mode networks. *Proc Natl Acad Sci USA*. Aug 26; 2008 105(34):12569–74. [PubMed: 18723676]
48. Garfinkel SN, Critchley HD. Interoception, emotion and brain: new insights link internal physiology to social behaviour. Commentary on: “Anterior insular cortex mediates bodily sensibility and social anxiety” by Terasawa et al. (2012). *Soc Cogn Affect Neurosci*. Mar; 2013 8(3):231–4. [PubMed: 23482658]
49. Reynolds SM, Zahm DS. Specificity in the projections of prefrontal and insular cortex to ventral striatopallidum and the extended amygdala. *J Neurosci*. Dec 14; 2005 25(50):11757–67. [PubMed: 16354934]
50. Salvador R, Martínez A, Pomarol-Clotet E, Gomar J, Vila F, Sarró S, et al. A simple view of the brain through a frequency-specific functional connectivity measure. *Neuroimage*. Jan 1; 2008 39(1):279–89. [PubMed: 17919927]
51. Garcia R, Spennato G, Nilsson-Todd L, Moreau J-L, Deschaux O. Hippocampal low-frequency stimulation and chronic mild stress similarly disrupt fear extinction memory in rats. *Neurobiol Learn Mem*. May; 2008 89(4):560–6. [PubMed: 18039585]
52. Sotres-Bayon F, Sierra-Mercado D, Pardilla-Delgado E, Quirk GJ. Gating of fear in prelimbic cortex by hippocampal and amygdala inputs. *Neuron*. Nov 21; 2012 76(4):804–12. [PubMed: 23177964]
53. Lissek S, Bradford DE, Alvarez RP, Burton P, Espensen-Sturges T, Reynolds RC, et al. Neural substrates of classically conditioned fear-generalization in humans: a parametric fMRI study. *Soc Cogn Affect Neurosci*. Jul 16.2013
54. Greicius MD, Flores BH, Menon V, Glover GH, Solvason HB, Kenna H, et al. Resting-state functional connectivity in major depression: abnormally increased contributions from subgenual cingulate cortex and thalamus. *Biol Psychiatry*. Sep 1; 2007 62(5):429–37. [PubMed: 17210143]
55. Shehzad Z, Kelly AMC, Reiss PT, Gee DG, Gotimer K, Uddin LQ, et al. The resting brain: unconstrained yet reliable. *Cereb Cortex*. Oct; 2009 19(10):2209–29. [PubMed: 19221144]
56. Birn RM, Molloy EK, Patriat R, Parker T, Meier TB, Kirk GR, et al. The effect of scan length on the reliability of resting-state fMRI connectivity estimates. *Neuroimage*. Dec.2013 83:550–8. [PubMed: 23747458]
57. Philip NS, Sweet LH, Tyrka AR, Price LH, Bloom RF, Carpenter LL. Decreased default network connectivity is associated with early life stress in medication-free healthy adults. *Eur Neuropsychopharmacol*. Jan; 2013 23(1):24–32. [PubMed: 23141153]
58. Bluhm RL, Williamson PC, Osuch EA, Frewen PA, Stevens TK, Boksman K, et al. Alterations in default network connectivity in posttraumatic stress disorder related to early-life trauma. *J Psychiatry Neurosci*. May; 2009 34(3):187–94. [PubMed: 19448848]



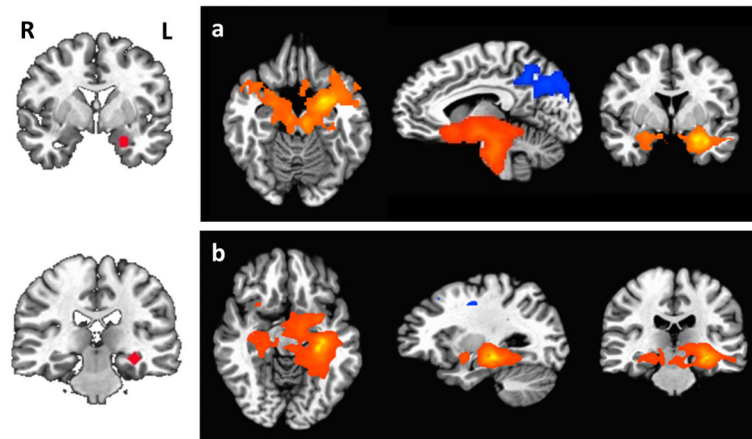


**Figure 1.**

Functional connectivity maps showing regions that are significantly connected to a) left amygdala, and b) left hippocampus. Seed regions are shown on the left, with connectivity maps on the right. Connectivity maps for the right amygdala and hippocampus showed similar patterns. Positive connectivity is indicated by orange-yellow overlays, and negative connectivity by blue overlays. For axial and coronal views, the right side of the brain faces left. Maps are displayed at voxelwise  $p = 0.005$ .

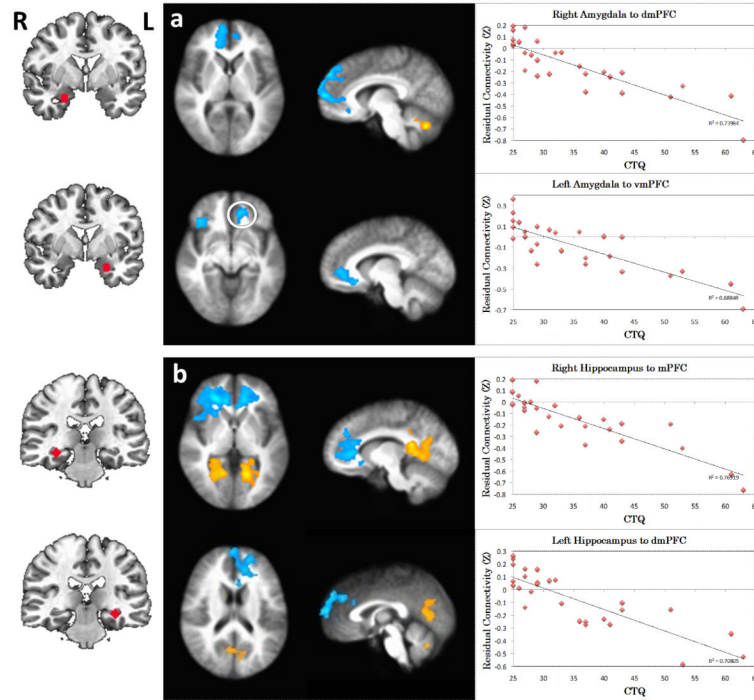


**Figure 2.** Correlation between childhood maltreatment (CTQ) and resting functional connectivity of the a) amygdala and b) hippocampus. The images in the middle indicate the brain areas where the connectivity to the seed region (shown on the left) is significantly correlated with CTQ ( $p < 0.05$ , corrected). Positive correlations are indicated by orange-yellow overlays, and negative correlations with blue overlays. For axial and coronal views, the right side of the brain faces left. Scatterplots on the right show the relationship between CTQ and the extracted, residualized connectivity values for the functional regions of interest. CTQ=Childhood Trauma Questionnaire, total score.

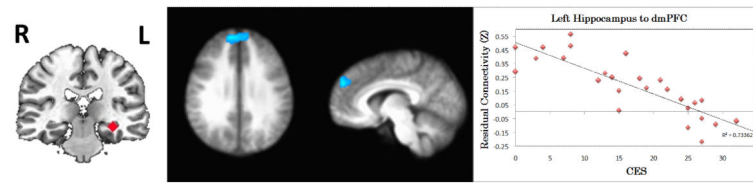


**Figure 3.**

Correlation between combat exposure (CES) and resting functional connectivity of the hippocampus. The images in the middle indicate the brain areas where the connectivity to the seed region (shown in the left figure) is significantly correlated with CES ( $p < 0.05$ , corrected). Positive correlations are indicated by orange-yellow overlays, and negative correlations with blue overlays. For axial and coronal views, the right side of the brain faces left. The scatterplot on the right shows the relationship between CES and the extracted, residualized connectivity values for the functional region of interest. CES=Combat Exposure Scale.

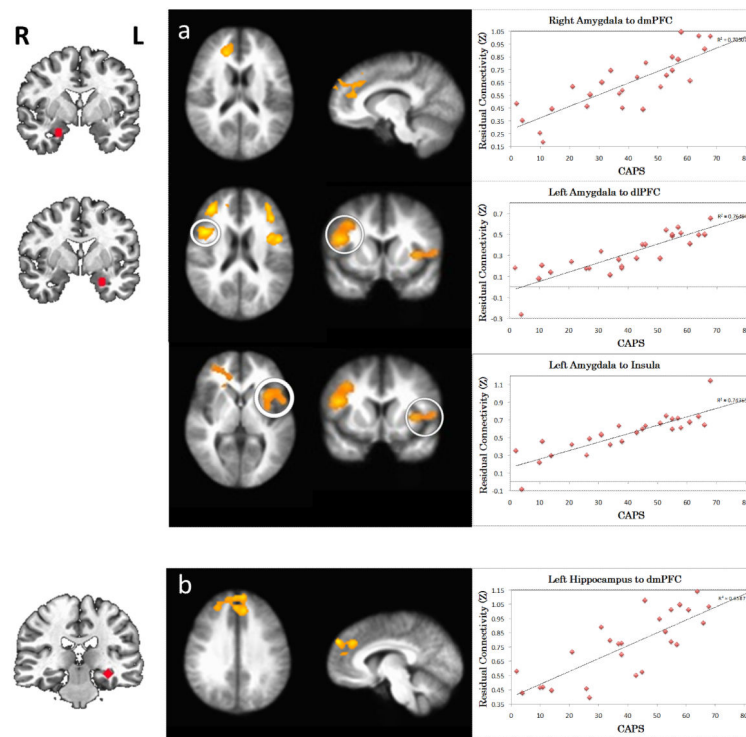


**Figure 4.** Correlation between post-traumatic stress symptoms (PTSS) and resting functional connectivity of the a) amygdala and b) hippocampus. The images in the middle indicate the brain areas where the connectivity to the seed region (shown on the left) is significantly correlated with PTSS ( $p < 0.05$ , corrected). Positive correlations are indicated by orange-yellow overlays, and negative correlations with blue overlays. For axial and coronal views, the right side of the brain faces left. Scatterplots on the right show the relationship between CAPS and the extracted, residualized connectivity values for the functional regions of interest. PTSS were based on the past month total score of the Clinician-Administered PTSD Scale (CAPS).

**Table 1**

Summary of prior resting state functional connectivity studies of childhood stress/trauma, and adult PTSD symptoms. Studies included here assessed one or more key fear network nodes including the amygdala, hippocampus, and/or prefrontal cortex. Note that decreases in connectivity that originally have a negative sign reflect a loss of anticorrelation.

Childhood Stress/Trauma Exposure						
Ref.	Seed or Network Analysis	Seed/Network Approach	Stress/Trauma Type	Subjects (n)	Main Findings (original connectivity sign)	Notes
13	Seed	Amygdala dACC PCC dmPFC	Childhood emotional maltreatment (CEM) – emotional abuse/neglect	Adults with CEM (44) Adults without CEM (44)	↓Amygdala-insula/hippocampus (+) ↓Amygdala-precuneus (-) ↓dACC-vmPFC (+) ↓dACC-precuneus (-)	Psychiatric medication use not reported. Groups matched for psychopathology. Physical/sexual abuse excluded.
14	Seed	Amygdala	Maternal/family stress up to 1 year of age	Adolescent community sample (57)	↓Amygdala-vmPFC (+)	Effects found in females only and mediated by child cortisol levels at age 4.5 years.
15	Seed	Amygdala Hippocampus	Childhood maltreatment – all types combined	Adolescent community sample (64)	↓Amygdala-sgACC (+) ↓Hippocampus-sgACC (+)	Amygdala effects in females only, hippocampus effects in both sexes.
57	Seed	Amygdala PCC	Childhood maltreatment (CM) – physical, sexual, or emotional abuse	Healthy adults with CM (12) Healthy adults without CM (9)	↓PCC-vmPFC (+) ↓PCC-ITC (+) ↑Amygdala-vmPFC (trend only)	A priori search regions were used. All subjects were free of current psychiatric illness. Four adults with CM reported past psychiatric illness.
16	Network	Graph theory	Childhood neglect (CN) – emotional/physical	Adult MDD with CN (18) Adult MDD without CN (20) Healthy adults without CN (20)	MDD with vs. without CN: ↓global connectivity in dl/vl/dmPFC, insula, caudate, thalamus, parahippocampal gyrus, amygdala, hippocampus	All MDD patients were receiving antidepressant medications. Primary analysis used global signal regression. Most CN-associated findings disappear when global signal regression was not used. Global connectivity = degree.
17	Network	Graph theory	Early life stress (ELS) such as abuse, neglect, caregiver death, accident	“Susceptible” adults with current or past MDD/PTSD and ELS (19) “Resilient” adults (no MDD/PTSD) with ELS (7) “Control” adults without ELS (12)	Susceptible vs. other groups: ↓local connectivity and ↑hub properties of amygdala, ↓hub properties of dACC, ↓local connectivity of left vlPFC Resilient vs. other groups: ↓global connectivity and hub properties of right vlPFC, ↓local	All female sample. Only ↓hub properties of right vlPFC for the resilient group survives multiple comparison correction. Local connectivity = efficiency. Hub properties = betweenness centrality. Global connectivity = degree.

Childhood Stress/Trauma Exposure						
Ref.	Seed or Network Analysis	Seed/Network Approach	Stress/Trauma Type	Subjects (n)	Main Findings (original connectivity sign)	Notes
					connectivity of dACC, ↑local connectivity of mPFC, ↑global connectivity of hippocampus	
Adult PTSD						
58	Seed	PCC mPFC	Childhood abuse	PTSD (17) NTC (15)	↓PCC to mPFC, parietal cortex, middle temporal gyrus, parahippocampal gyrus, insula, hippocampus, amygdala ↓mPFC to parietal cortex, PCC	All female sample. Thirteen PTSD subjects were receiving psychiatric medications.
6	Seed	Amygdala	Combat	PTSD (17) TEC (17)	↑Amygdala-insula (+)	All male sample. PTSD subjects were unmedicated at time of study.
7	Seed	Amygdala	Combat	PTSD (15) TEC (14)	↑Amygdala-insula (+) ↓Amygdala-hippocampus (+) ↓Amygdala-rostral/dorsal ACC (-)	A priori search regions were used. All male sample. Two PTSD subjects were taking trazodone.
8	Seed	PCC vmPFC Anterior insula	Combat	PTSD (15) TEC (15) NTC, community sample (15)	PTSD vs. TEC: ↑PCC-amygdala and -insula (-) ↑Insula-amygdala (+) ↑Insula-hippocampus (-) PTSD vs. NTC: ↓PCC-hippocampus (+) ↓vmPFC-rostral ACC (+)	A priori search regions were used. All male sample. Two PTSD subjects were taking trazodone. The two comparison groups were combined for primary analysis
10	Seed	Anterior hippocampus Posterior hippocampus	Various – interpersonal violence, accident, combat, childhood abuse, rape, natural disaster	PTSD (17) GAD (39) NTC (60)	PTSD vs. NTC: ↓Anterior hippocampus to dACC/pre-SMA (+) ↓Posterior hippocampus to PCC, PC, pgACC (+)	A priori search regions and global signal regression were used. Four PTSD subjects were receiving psychiatric medications. Posterior hippocampal findings were specific to PTSD.
9	Seed	Basolateral amygdala (BLA) Centromedial amygdala (CMA)	Combat	PTSD (20) TEC (22)	↓BLA-pgACC/dmPFC (-) ↓BLA-dACC (-) ↓BLA to IFG (+)	Twelve PTSD and two TEC subjects were receiving psychiatric medications.



**Table 2**

Regression analysis results using seed connectivity and behavioral measures. Positive or negative correlations with each clinical variable and seed connectivity are indicated by + or – and were significant at  $p < 0.05$  corrected. “Original raw connectivity” describes the sign of the raw connectivity between the ROI seed and the cluster of interest.

Behavior Scale	Seed	Cluster Location	Brodmann Areas	Original Raw Connectivity	x	y	z	Peak Z	Cluster voxels
CTQ									
+	L.Amyg	R. Cerebellum	–	Positive *	–14	42	–30	6.66	718
	R.Amyg	R. Cerebellum	–	Negative (close to zero)	–10	66	–30	6.93	2966
	L.Hip	L. Cerebellum	–	Negative	10	78	–28	5.41	487
	L.Hip	PCC / Precuneus	30, 31	Positive *	–30	48	0	5.13	1702
	R.Hip	PCC / Precuneus	30, 31	Positive (close to zero)	–12	38	12	6.42	3892
–	L.Amyg	R. vIPFC / dIPFC	47, 10 / 9	Negative (close to zero)	–36	–40	24	–5.89	980
	L.Amyg	L. rACC	10, 32	Negative	10	–40	–6	–4.8	953
	R.Amyg	R.mPFC	9, 10, 32	Negative	–10	–62	10	–5.92	2439
	R.Amyg	L. SOG	19	Negative (close to zero)	32	82	34	–5.55	398
	L.Hip	L. mPFC	9, 10, 32	Positive	10	–36	2	–5.76	2634
	R.Hip	R.lPFC	10, 46	Negative	–24	–38	2	–6.13	2659
	R.Hip	L.rACC	10, 32	Negative *	16	–42	20	–6.38	2013
R.Hip	R.dIPFC	8, 9	Negative (close to zero)	–34	–30	40	–5.21	375	
CES									
+	R.Amyg	L. Cerebellum	–	Positive (close to zero)	18	58	–28	5.33	394
–	L.Hip	R.dmPFC	9	Negative	–8	–54	32	–5.63	537
CAPS									
+	L. Amyg	L.Ins / L. FO	13 / 9, 44	Positive (close to zero)	48	–2	20	5.64	1486
	L. Amyg	R.dIPFC	10, 46	Negative	–34	–40	26	7.49	892
	L. Amyg	R.Ins / R.FO	9, 44 / 9, 13	Positive (close to zero)	–44	–12	20	6.03	692
	L. Amyg	L.dIPFC	10, 46	Negative (close to zero)	38	–30	20	5.1	371
	R.Amyg	R.dmPFC	9, 32	Negative	–18	–36	18	4.96	766
	L.Hip	dmPFC	9	Negative (close to zero)	6	–56	34	5.61	757
–	L.Amyg	R. Cerebellum	–	Positive *	–14	26	–30	–6.25	462
	L.Hip	PCC	30	Positive *	–16	58	8	5.29	564

\* significant original raw connectivity between the regions ( $p < 0.05$  corrected). Amyg = Amygdala, Ins = Insula, mPFC = medial prefrontal cortex, Hip = hippocampus, PCC = posterior cingulate cortex, dlPFC = dorsolateral prefrontal cortex, dmPFC = dorsomedial prefrontal cortex, lPFC = lateral prefrontal cortex, rACC = rostral cingulate cortex, SOG = superior occipital gyrus, FO = frontal operculum.